Testing a Laser Setup to Measure Surface Flatness

A thesis submitted in partial fulfillment of the requirement
for the degree of bachelor of science in physics
from the College of William and Mary in Virginia,

by

Brett Appleton.

Accepted for_____

_____
Advisor:

_____

_____

_____

_____

Williamsburg, Virginia
July 2006

1

Abstract

An experiment has been proposed and approved at Jefferson Lab to make a high precision measurement of the proton's weak charge at low momentum transfer. The results of this experiment will be used in part to confirm or reject certain predictions of the standard model of particle physics. The experimental setup includes drift chambers which will be constructed at the College of William and Mary. The main goal of this project is to develop a laser setup that will allow for precision measurement of the topography of the wire frames within these drift chambers. The proposed laser setup is seen to have accuracy (≈1.68 μm) well within that required. When tested on a known surface it showed a 2% error in measuring the actual slope.

Contents

1 The Q$_{weak}$ Experiment

1.1 Motivations and Overview

The proposed Q$_{weak}$ experiment [1] to be conducted at The Thomas Jefferson National Accelerator Facility in Newport News Virginia will be the first high precision measurement of the weak charge of the proton, $Q_w^p = 1 - 4\sin^2\theta_w$, at low momentum transfer. One reason this will be an important experiment is that it can be used to test certain predictions of the Standard Model of particle physics. If these predictions of the Standard Model are not found to be consistent with experimental results then this could signal the presence of new physics beyond the Standard Model.

The prediction in question is that of the value of the weak mixing angle, $\sin^2\theta_w$, at different values of the four-momentum transfer, Q^2 [2]. This is commonly referred to as the running of $\sin^2\theta_w$. The Q$_{weak}$ experiment will allow for a very high precision calculation of $\sin^2\theta_w$ at a low value of Q^2, around 0.03 (GeV/c)^2. This experiment will observe the parity-violating elastic scattering of electrons off of a proton target. The asymmetry present in this scattering is given by

$$A_{LR} = \frac{\sigma_+ - \sigma_-}{\sigma_+ + \sigma_-}. \qquad (1)$$

Here σ_+ is the rate of detected scatterings by right-handed electrons and σ_- is the rate of detected scatterings by left-handed electrons. That is, there is an asymmetry in the probability that right-handed versus left-handed electrons will be scattered. This observed asymmetry can then be used to determine the weak charge of the proton.

$$A_{LR} = -\frac{G_F Q^2}{4\sqrt{2}\pi\alpha}\left[Q_w^p + F^p\left(Q^2, \theta\right)\right] \qquad (2)$$

where G_F is the Fermi constant, α is the fine structure constant and F^p is a proton structure-dependent form factor. Since the contributions of the form factor F^p are negligible at low values of Q^2, A_{LR} is approximately proportional to $Q^2 Q^p_w$ [3].

In order to determine Q^p_w from a measurement of A_{LR}, it is necessary to know the kinematics of the experiment, i.e. Q^2, precisely. This will be accomplished in the Q_{weak} experiment through the use of drift chambers.
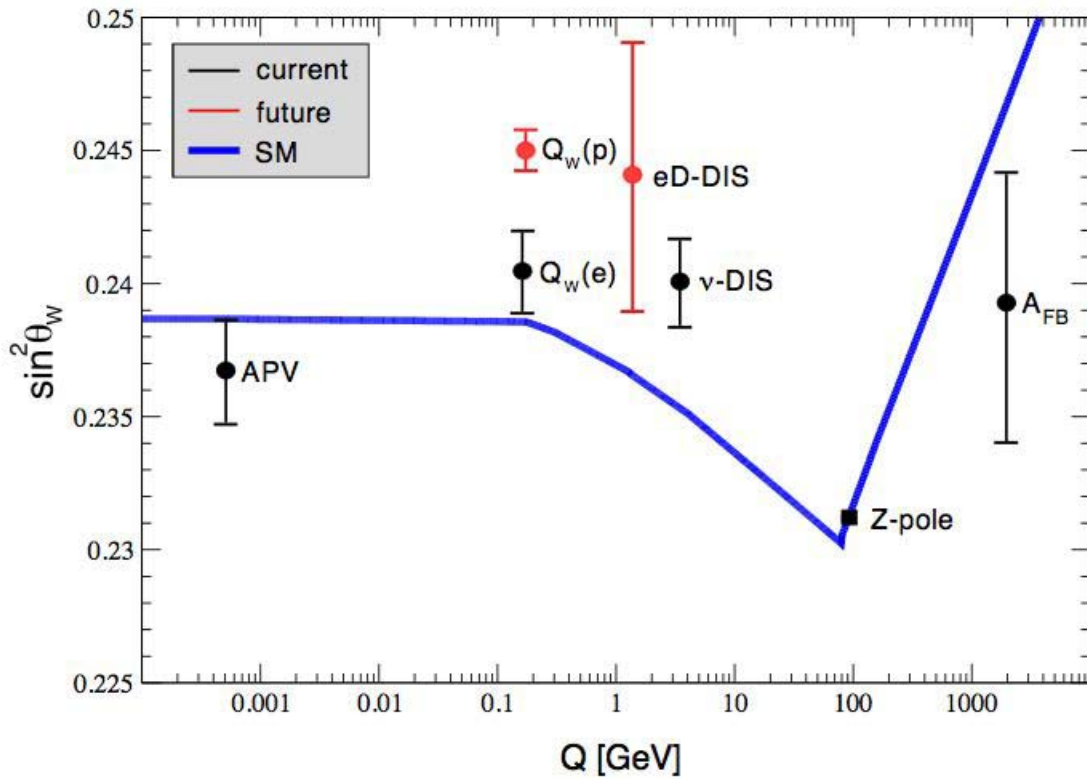

Figure 1.1.1 – The blue line represents the theoretically predicted relation between the weak mixing angle and the value of Q^2. The other points represent either published or proposed measurements of this relation. The red bars are anticipated error bars which are arbitrarily located vertically. [4]

1.2 Methods

The Q_{weak} experiment will employ a 2200 hour measurement of the parity-violating asymmetry observed from the scattering of electrons from a 35 cm liquid Hydrogen target.

Elastically scattered electrons at $Q^2 \approx 0.03$ GeV^2 will be directed towards a set of eight

quartz Cerenkov detectors by a toroidal magnet. These detectors will be viewed by

photomultiplier tubes which will allow the detection of electrons incident on the Cerenkov
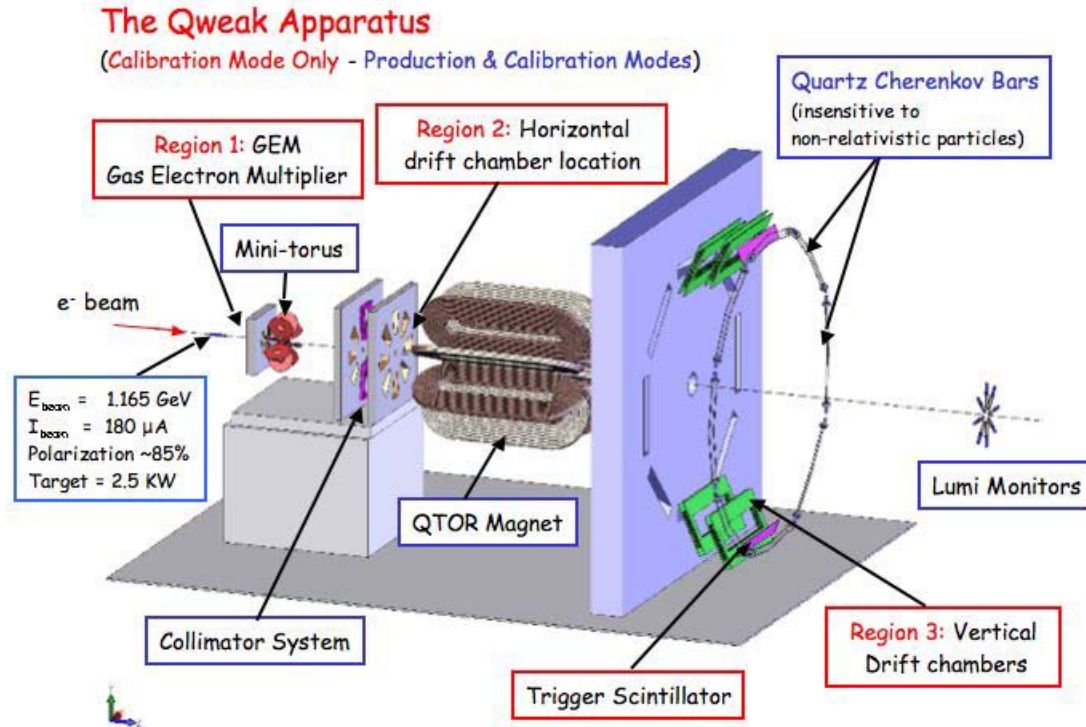
detectors [1].

Figure 1.2.1 – Depiction of the Q$_{weak}$ apparatus to be constructed at Jefferson Lab. [4]

1.3 Parity Violation

The parity operator, P, is an operator that reverses the sign of the three coordinate

axes, that is, $P{:}(x, y, z) \rightarrow (-x, -y, -z)$. Ψ is said to be parity conserving if it is an eigenstate of

P, that is, if $P\Psi = \pm\Psi$. Otherwise Ψ is said to violate parity. The force of gravity, for

example, is parity conserving since it depends only on the distance between objects.

However, any interactions that depend on the spin of particles could be parity violating [5].

Whereas electromagnetic forces do not distinguish between left-handed and right-handed particles, these particles will behave differently under the influence of the weak force. It is because of this fact that the weak force is parity violating that the asymmetry given by equation (1) arises.

Because the weak force is parity violating, the number of left-handed electrons that are elastically scattered will be slightly different from the number of right-handed electrons that are elastically scattered. Thus, the Cerenkov detectors will actually see this parity violation and provide a value for A_{LR}. This will then allow for the calculation of the weak mixing angle and the proton's weak charge.

1.4 Drift Chambers

The purpose of a drift chamber is to aid in the reconstruction of a particle's path or point of origin. The basic design of a drift chamber is a collection of wire planes inside of a gas filled chamber with an applied electric field. As an electron travels through the drift chamber it ionizes the gas causing the appearance of secondary electrons within the drift chamber. These secondary electrons can then cause secondary ionization. As this process continues, an avalanche effect occurs, meaning that there will be a large number of electrons traveling towards the wires in the wire planes as the initial electron continues on its path through the drift chamber.
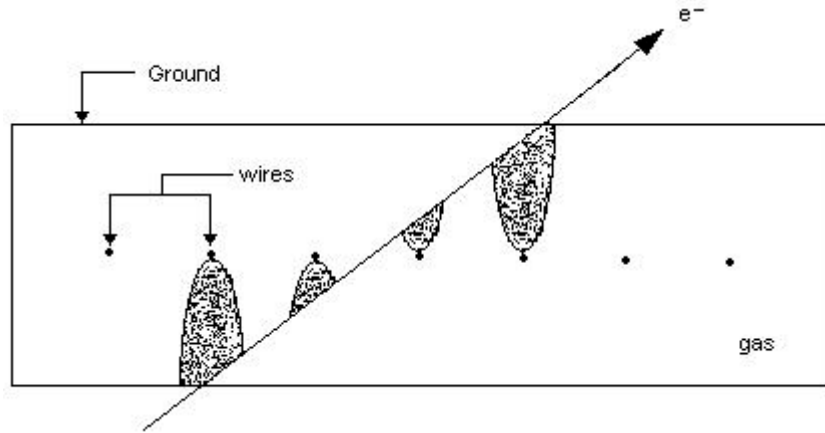
Figure 1.4.1 – As an electron passes through the drift chamber, it causes an avalanche effect which sends multiple electrons drifting towards the wire planes of the drift chamber.

In the Q$_{weak}$ experiment drift chambers will be used to help determine the path of electrons. Since both the drift velocity of electrons in the gas and the arrival time of an avalanche at a particular wire are known, the distance of a scattered electron's path from that wire can be deduced. By looking at how far the scattered electron's path is from multiple wires, a precise picture of that electron's path can be constructed.

2 The Experiment

The main focus of this project was to develop and test a laser system to measure surface flatness. In terms of the Q$_{weak}$ experiment this system will be used during the construction of the vertical drift chambers to measure the flatness of frames for each wire plane. Since these drift chambers are essential to a precise calculation of Q^2, the E-field inside these chambers must be known. In order to know what the E-fields look like it is necessary to know very precisely the locations of the wires. By using this system to detect any deviations from flatness in the frames, such knowledge of the locations of the wires can be obtained.

2.1 Our setup

Our setup consisted of a laser transmitter and receiver (A-LAS 12/90) along with an

electronic control unit (AGL4-…-HS) produced by Sensor Instrument GmbH. The

transmitter emits a rectangular beam with linear beam profile and λ=670 nm. The

maximum power output is 1 mW. The maximum working range of 10 m is acceptable

since the wire frames are no longer than eight feet.

      Figure 2.1.1 shows the basic setup of this laser system. The sender and receiver are

aligned so that a maximum output voltage is obtained. Precision gauge blocks are then

placed at various points along the beam so that part of the beam is blocked. A change in the

output voltage as the block is moved signals a change in the fraction of the beam being

blocked. This means that there is some deviation from flatness in the surface on which the
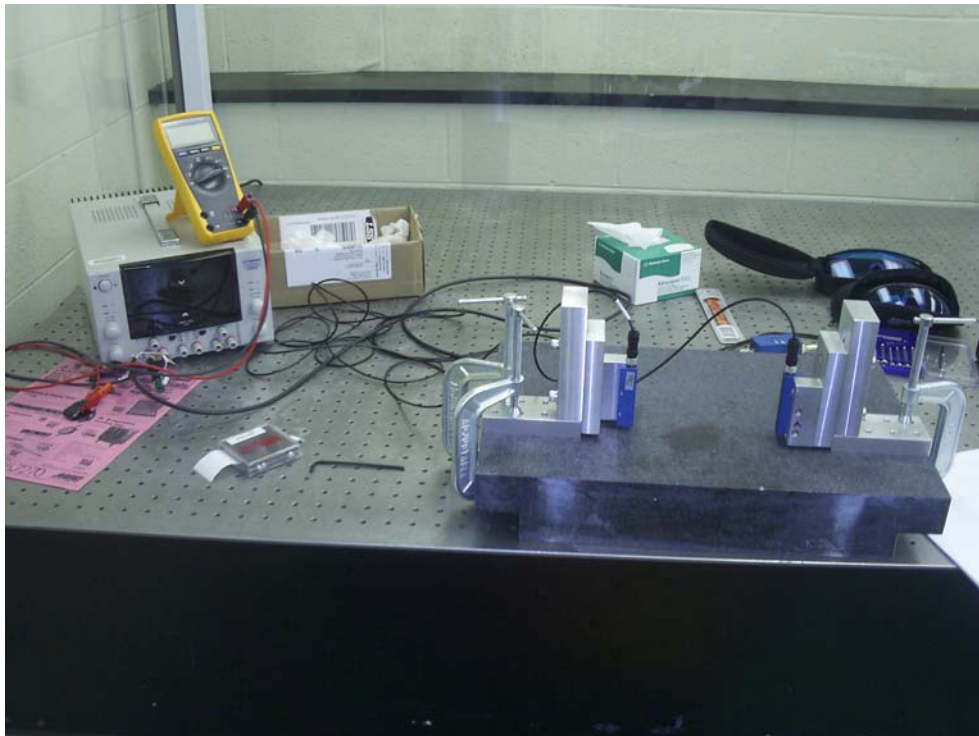
gauge block is sitting on.

Figure 2.1.1 – Photo of our setup for testing the capabilities of the laser
system to provide information on height variation.

      The output voltage of the receiver was measured with a Fluke 175 true RMS

multimeter with a resolution of 1 mV. The granite table used during calibration and testing

of this system was known to be flat to within ±0.27 µm. The initial setup allowed for only

coarse height adjustment of the laser and receiver. The sensitivity of the receiver to

ambient light was found to be at the 1 mV (~0.33 µm) level. The beam profile was

measured four times using this setup by aligning the laser and receiver and then placing

various height gauge blocks in the path of the beam (section 4.1). These results showed

good linearity of the beam profile but also showed some variability of the slope. The

average slope of four trials was -3.037 mV/µm. By placing the same gauge block in the

path of the laser 20 times the accuracy of the system was found to be at the level of 11.1 µm
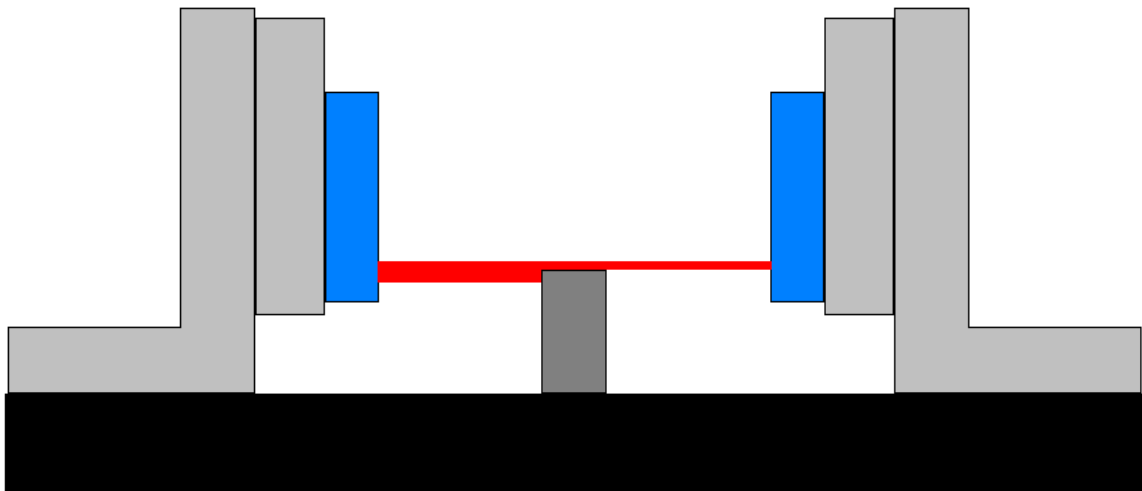
(section 4.5).

Figure 2.1.2 – Schematic of the working laser system with the laser on
the left.

However, when this setup was used to measure the flatness of the granite table, it

was found that the laser and receiver were not properly aligned due to tilting (section 4.2).

The output voltage was 4.2 V when the gauge block was placed near the receiver and it

dropped to 3.341 V as the block was moved next to the sender. In order to reduce this

problem new mounting blocks were constructed for the laser and the receiver. These new

blocks included precision screws to adjust the tilt of the laser and the receiver as well as a translation stage to finely adjust both the vertical and horizontal position of the laser. These new mounts allowed for much more precise alignment of the laser and receiver. The new procedure consisted of doing a coarse height adjustment first and then the fine vertical and horizontal adjustments. Next the screws can be used to adjust the tilt of the laser. However, once the tilting angle is close enough to zero, the vertical and horizontal positions must be rechecked.

The beam profile was measured three more times using this new setup (section 4.3). Each time the system was realigned and then gauge blocks were placed in the path of the beam. These results continued to show good linearity as well as much less variability of the slope than did the measurements with the initial setup. These trials had a variation of 0.040 mV/μm whereas the initial trials had a variation of 0.161 mV/μm. The average slope of the three trials with the new setup was -3.341 mV/μm. By placing the same gauge block in the path of the laser 20 times the accuracy of the system was found to be at the level of 1.68 μm (section 4.5).

The laser system was then used to measure a known non-flat surface (section 4.4). Two precision parallels along with a 0.05 inch gauge block were used to create a surface with known slope of 0.0097. A gauge block was then placed every half inch along the length of the surface and the output voltage was recorded for each position. The calculated slope was 0.0099.

3 Conclusions

This laser system with the current mounting blocks is capable of measuring surface flatness to the precision required (~25 µm). Based on the repositioning of a single block the accuracy has been estimated to be better than 2 µm. Although there was a 2% error in the calculation of the slope of the known non-flat surface, the movement of the gauge block during this test was somewhat imprecise.

It would be useful however to test again the time stability of the output with the new setup to see if it is any better than that with the initial setup. It would also be nice to do a second measurement of the flatness of the granite table with the new setup to see if it really shows a horizontal line with height variation at the 0.27 µm level.

4 Tables of Results

4.1 Initial height data

Trial 1:

Block Height (in)	Output (Volts)	Block Height (in)	Output (Volts)	Block Height (in)	Output (Volts)	Block Height (in)	Output (Volts)	Block Height (in)	Output (Volts)	Block Height (in)	Output (Volts)
0.36	8.95	0.375	8.72	0.39	7.57	0.405	6.508	0.42	5.193	0.435	3.976
0.361	8.95	0.376	8.66	0.391	7.47	0.406	6.416	0.421	5.123	0.436	3.954
0.362	8.94	0.377	8.58	0.392	7.4	0.407	6.329	0.422	5.044	0.437	3.874
0.363	8.94	0.378	8.5	0.393	7.32	0.408	6.233	0.423	4.982	0.438	3.765
0.364	8.93	0.379	8.42	0.394	7.22	0.409	6.143	0.424	4.914	0.439	3.695
0.365	8.93	0.38	8.33	0.395	7.14	0.41	6.053	0.425	4.848	0.44	3.637
0.366	8.92	0.381	8.26	0.396	7.09	0.411	5.946	0.426	4.774	0.441	3.563
0.367	8.92	0.382	8.19	0.397	7.01	0.412	5.83	0.427	4.705	0.442	3.491
0.368	8.92	0.383	8.1	0.398	6.94	0.413	5.747	0.428	4.626	0.443	3.411
0.369	8.91	0.384	8.05	0.399	6.83	0.414	5.642	0.429	4.555	0.444	3.297
0.37	8.89	0.385	7.96	0.4	6.79	0.415	5.562	0.43	4.474	0.445	3.223
0.371	8.88	0.386	7.89	0.401	6.76	0.416	5.491	0.431	4.386	0.446	3.103
0.372	8.85	0.387	7.82	0.402	6.73	0.417	5.423	0.432	4.288	0.447	3.035
0.373	8.82	0.388	7.73	0.403	6.66	0.418	5.347	0.433	4.208	0.448	2.977
0.374	8.78	0.389	7.65	0.404	6.593	0.419	5.273	0.434	4.13	0.449	2.875

Trial 1 continued:

Block Height (in)	Output (Volts)	Block Height (in)	Output (Volts)	Block Height (in)	Output (Volts)	Block Height (in)	Output (Volts)
0.45	2.77	0.465	1.593	0.48	0.506	0.495	0.025
0.451	2.697	0.466	1.522	0.481	0.425	0.496	0.025
0.452	2.62	0.467	1.468	0.482	0.318		
0.453	2.525	0.468	1.403	0.483	0.256		
0.454	2.453	0.469	1.332	0.484	0.17		
0.455	2.375	0.47	1.247	0.485	0.089		
0.456	2.233	0.471	1.166	0.486	0.072		
0.457	2.197	0.472	1.051	0.487	0.045		
0.458	2.107	0.473	0.966	0.488	0.039		
0.459	2.027	0.474	0.898	0.489	0.034		
0.46	1.94	0.475	0.833	0.49	0.03		
0.461	1.87	0.476	0.752	0.491	0.028		
0.462	1.799	0.477	0.695	0.492	0.026		
0.463	1.736	0.478	0.629	0.493	0.025		
0.464	1.661	0.479	0.582	0.494	0.025		

Trial 2

Block Height (in)	Output (Volts)
none	8.51
0.4	8.51
0.41	8.51

Trial 3

Block Height (in)	Output (Volts)
none	8.31
0.5	8.31
0.51	8.31

Trial 4

Block Height (in)	Output (Volts)
none	8.62
0.15	8.62
0.16	8.62

Trial 2 cont.		Trial 3 cont.		Trial 4 cont.	
Block Height (in)	Output (Volts)	Block Height (in)	Output (Volts)	Block Height (in)	Output (Volts)
0.42	8.51	0.52	8.31	0.17	8.62
0.43	8.5	0.53	8.3	0.18	8.61
0.44	8.32	0.54	8.19	0.19	8.47
0.45	7.56	0.55	7.47	0.2	7.75
0.46	6.8	0.56	7.03	0.21	6.95
0.47	6.119	0.57	5.975	0.22	6.252
0.48	5.187	0.58	5.081	0.23	5.307
0.49	4.458	0.59	4.347	0.24	4.567
0.5	3.61	0.6	3.57	0.25	3.782
0.51	2.871	0.61	2.828	0.26	3.009
0.52	2.081	0.62	2.074	0.27	2.198
0.53	1.381	0.63	1.395	0.28	1.513
0.54	0.689	0.64	0.727	0.29	0.794
0.55	0.048	0.65	0.112	0.3	0.164
0.56	0.023	0.66	0.024	0.31	0.023

Trial 1

$y = -79.637x + 38.652$

$R^2 = 0.9996$

-3.135 mV/µm

Trial 2

$y = -76.486x + 41.954$

$R^2 = 0.9991$

-3.011 mV/µm

Trial 3

$y = -75.535x + 49.01$

$R^2 = 0.9975$

-2.974 mV/µm

Trial 4

$y = -76.915x + 23.074$

$R^2 = 0.9992$

-3.028 mV/µm
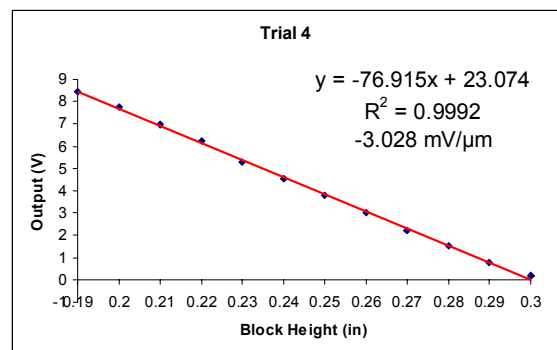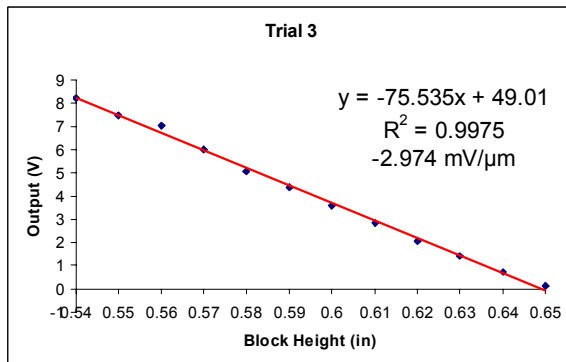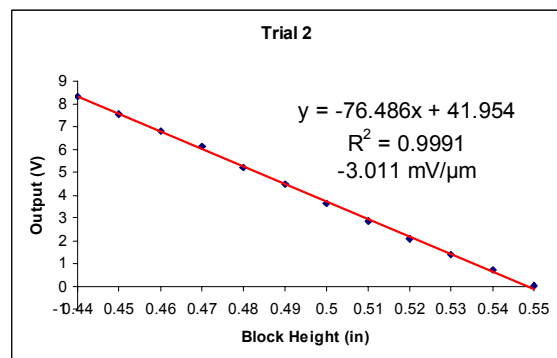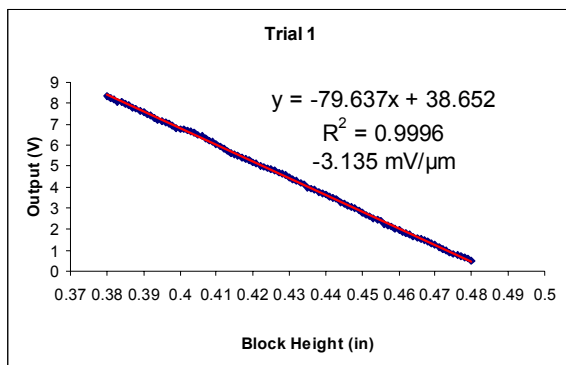
4.2 Initial granite table flatness

distance from receiver (in)	output (Volts)
0.25	4.2
0.5	4.157
0.75	4.122
1	4.065
1.25	4.009
1.5	3.961
1.75	3.912
2	3.864
2.25	3.825
2.5	3.779
2.75	3.738
3	3.698
3.25	3.669
3.5	3.633
3.75	3.596
4	3.558
4.25	3.521
4.5	3.489
4.75	3.447
5	3.419
5.25	3.385
5.5	3.341

$y = -0.1624x + 4.2119$
$R^2 = 0.9944$
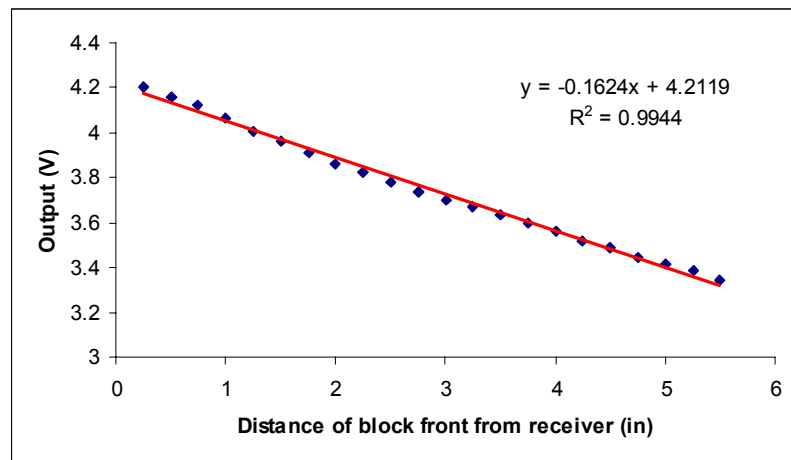
4.3 Height data with new setup

Trial 1		Trial 2		Trial 3	
Block Height (in)	Output (Volts)	Block Height (in)	Output (Volts)	Block Height (in)	Output (Volts)
none	9.43	none	9.44	none	9.44
1.27	9.43	1.27	9.44	1.27	9.44
1.28	9.43	1.28	9.41	1.28	9.44
1.29	8.97	1.29	8.81	1.29	9.43
1.3	8.23	1.3	8.03	1.3	9.04
1.31	7.37	1.31	7.21	1.31	8.19
1.32	6.303	1.32	6.319	1.32	7.37
1.33	5.537	1.33	5.399	1.33	6.534
1.34	4.705	1.34	4.572	1.34	5.63
1.35	3.845	1.35	3.677	1.35	4.766
1.36	3.004	1.36	2.856	1.36	3.804
1.37	2.164	1.37	1.979	1.37	3.05
1.38	1.337	1.38	1.253	1.38	2.181
1.39	0.647	1.39	0.533	1.39	1.441
1.4	0.076	1.4	0.066	1.4	0.681
1.41	0.056	1.41	0.056	1.41	0.082
1.42	0.056	1.42	0.056	1.42	0.056

Trial 1

$y = -84.625x + 118.14$
$R^2 = 0.9989$
$-3.331 \text{ mV/}\mu\text{m}$

Trial 2

$y = -84.482x + 117.81$
$R^2 = 0.9991$
$-3.326 \text{ mV/}\mu\text{m}$

Trial 3

$y = -85.52x + 120.22$
$R^2 = 0.9996$
$-3.366 \text{ mV/}\mu\text{m}$
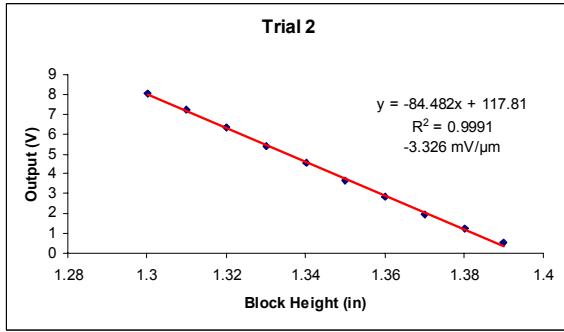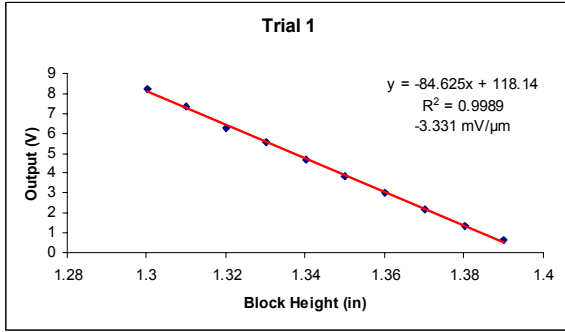
4.4 Measure known non-flat surface

Distance from end (µm)	Height (µm)
0	0
12700	140.7
25400	293.4
38100	416.2
50800	527
63500	658.2
76200	796.5
88900	923.4
101600	1029.4
114300	1141.4
127000	1257.3

measure known non-flat surface

$y = 0.0099x + 26.627$
$R^2 = 0.9984$
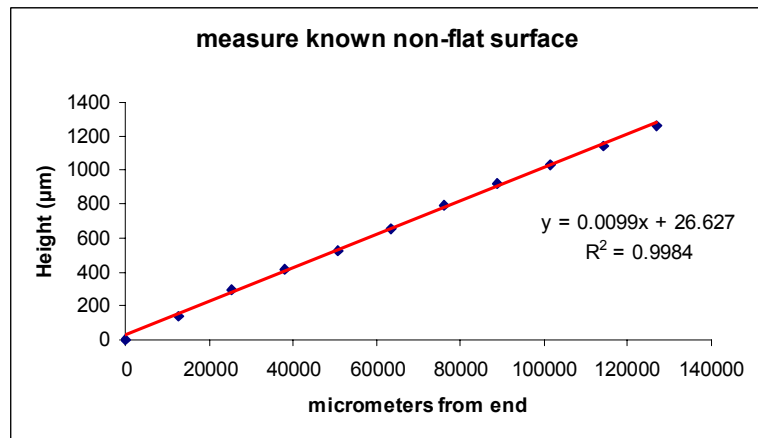
4.5 Single block reproducibility

	Initial setup		New setup
Trial	volts	Trial	volts
1	7.77	1	4.731
2	7.67	2	4.74
3	7.75	3	4.738
4	7.72	4	4.749
5	7.74	5	4.746
6	7.74	6	4.747
7	7.74	7	4.748
8	7.73	8	4.741
9	7.76	9	4.75
10	7.74	10	4.755
11	7.78	11	4.75
12	7.74	12	4.744
13	7.67	13	4.744
14	7.79	14	4.747
15	7.79	15	4.748
16	7.79	16	4.749
17	7.74	17	4.749
18	7.77	18	4.742
19	7.77	19	4.743
20	7.76	20	4.754
	$\sigma =$ 0.033811		$\sigma =$ 0.0056
	$\sigma =$ 11.1 µm		$\sigma =$ 1.68 µm

old setup
Normal

Mean 7.748
StDev 0.03381
N 20

new setup
Normal

Mean	4.746
StDev	0.005600
N	20
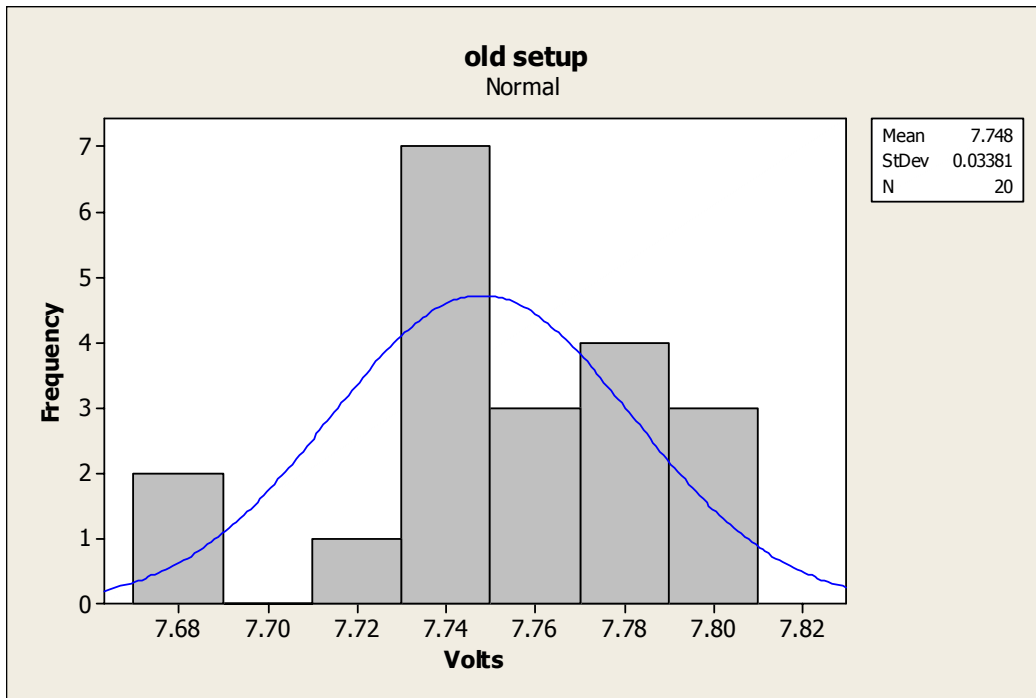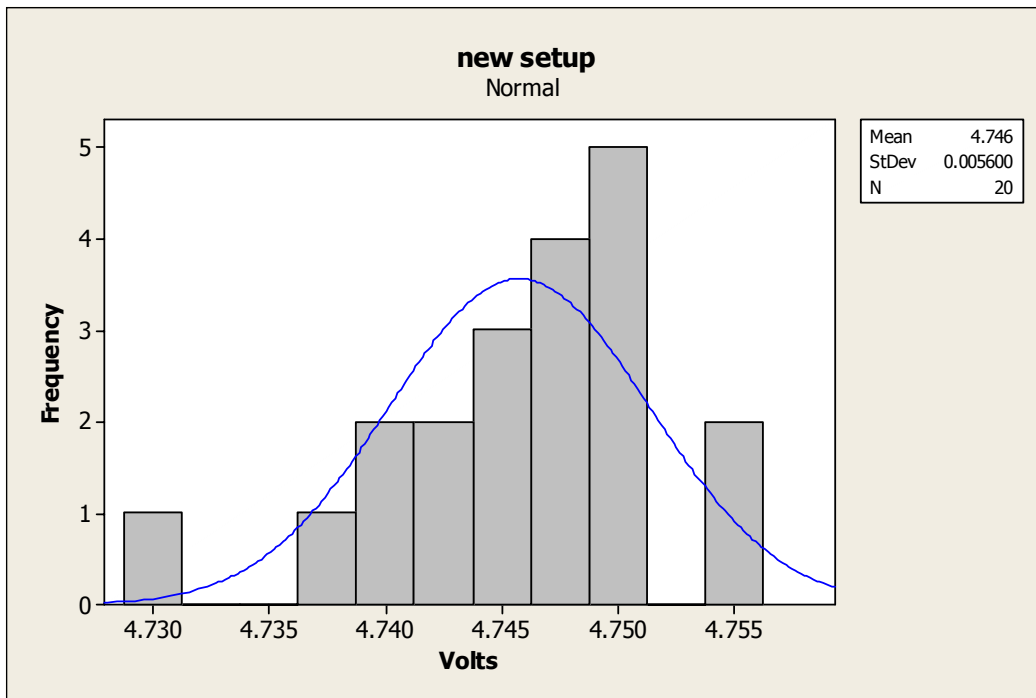
4.6 Time stability (done with initial setup)

12:53 PM – 8.70 Volts
2:35 PM – 8.73 Volts

5 References

[1] Armstrong, et al. "The Q_{weak} Experiment: A Search for New Physics at the TeV Scale Via a Measurement of the Proton's Weak Charge". Proposal to Jefferson Lab program advising committee. 3 Dec 2001.

[2] E. Epperson. "Software and Simulation for Q_{weak}". Senior Research Thesis. 16 April 2004.

[3] J. Erler, et al. "The Weak Charge of the Proton and New Physics". Caltech MAP-287. 17 Feb 2003.

[4] http://www.jlab.org/qweak/

[5] G. Garvey and J. Seestrom. "Parity Violation in Nuclear Physics". *Los Alamos Science*, Number 21, 1993. pp. 156-164.

[6] K. Kleinknecht. *Detectors for Particle Radiation*. Cambridge Univ. Press. 1990.